Chapter 19

The Rayleigh–Taylor and flute instabilities

In Chapter 9, we learned that magnetohydrodynamic plasma equilibria must be determined self-consistently, i.e. the presence of currents flowing in the plasma modifies the magnetic configuration in which the plasma rests. A static magnetohydrodynamic equilibrium (plasma fluid velocity $\mathbf{u} = 0$, hence electric field $\mathbf{E} = 0$) occurs when the plasma pressure gradients are balanced by magnetic ($\mathbf{j} \times \mathbf{B}$) forces.

However, even if a magnetohydrodynamic equilibrium exists in some particular case, the lack of *plasma stability* can lead to the spontaneous generation of $\mathbf{E}$ fields and associated plasma velocities $\mathbf{u}$. For if the plasma is disturbed slightly, its motion can deform the magnetic field in such a way as to produce magnetic forces that tend to amplify the original disturbance. This type of phenomenon is called a 'magnetohydrodynamic (MHD) instability'.

Because of the complexity of the magnetohydrodynamic equations, we are generally only able to treat analytically the case of *linear* stability, i.e. stability against *infinitesimally small* disturbances, in relatively simple geometries. For spatially uniform plasmas, infinitesimal perturbations will generally have a wave-like spatial structure. In such cases, as was discussed in Chapter 15, a plane wave with a single wave-vector $\mathbf{k}$ will generally have a single frequency ω. Thus, for a uniform plasma, this plane wave will be a 'normal mode'. For non-uniform plasmas, such as those considered in the present Chapter, it will be necessary to find the 'eigenfunctions', describing the spatial structure in the direction of non-uniformity, of the normal modes of perturbations, i.e. the modes which oscillate (or grow) with a single (possibly complex) frequency ω.

The theory of magnetohydrodynamic stability has been developed rigorously and applied analytically and numerically for a variety of plasmas using a variational principle, known as the 'MHD energy principle'. The MHD energy principle was formulated by I B Bernstein, E A Frieman, M D Kruskal and R M Kulsrud (1958 *Proc. R. Soc. (London)* A **744** 17). The energy principle

lies outside the scope of this book, however. Rather, we will limit ourselves to a simple configuration for which the normal modes can be obtained explicitly, and we will then use general arguments to extend our results qualitatively to other configurations.

19.1 THE GRAVITATIONAL RAYLEIGH–TAYLOR INSTABILITY

Perhaps the most important MHD instability is the Rayleigh–Taylor (or 'gravitational') instability. In ordinary hydrodynamics, a Rayleigh–Taylor instability arises when one attempts to support a heavy fluid on top of a light fluid: the interface becomes 'rippled', allowing the heavy fluid to fall through the light fluid. In plasmas, a Rayleigh–Taylor instability can occur when a dense plasma is supported against gravity by the pressure of a magnetic field.

The situation would not be of much interest or relevance in its own right, since actual gravitational forces are rarely of much importance in plasmas. However, in curved magnetic fields, the centrifugal force on the plasma due to particle motion along the curved field-lines acts like a 'gravitational' force. (Expressed differently, as we saw in Chapters 2 and 3, the electron and ion drifts due to magnetic-field gradient and curvature (∇B and curvature drifts) are similar to the particle drifts that arise from a gravitational field (gravitational drift).) For this reason, the analysis of the Rayleigh–Taylor instability provides useful insight as to the stability properties of plasmas in curved magnetic fields. Rayleigh–Taylor-like instabilities driven by actual field curvature are the most virulent type of MHD instability in non-uniform plasmas.

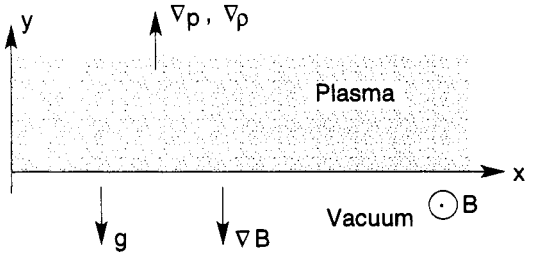

Figure 19.1. An equilibrium in which a plasma is supported against gravity by a magnetic field.

To treat the simplest case, we consider a plasma that is non-uniform in the y direction only and is immersed in a magnetic field in the z direction. To be specific, we suppose that the density gradient $\nabla\rho$ is in the y direction and that the gravitational field $\mathbf{g}$ is opposite to it, i.e. in the negative y direction. This corresponds to the case of a dense plasma supported against gravity by a magnetic field, as shown in Figure 19.1. Although Figure 19.1 suggests that

there is a sharp boundary between the plasma and the vacuum, this is only one possible case and is used here primarily for illustration; the density 'profile' $\rho_0(y)$ may, in practice, be a smoothly increasing function of y. For the purposes of our present analysis, we will assume that the density has an exponential shape in y, i.e.

$$\rho_0(y) \propto \exp(y/s) \tag{19.1}$$

where s denotes the density-gradient 'scale length'. The plasma is bounded by conducting walls at $y = 0$ and $y = h$. This is illustrated in Figure 19.2.

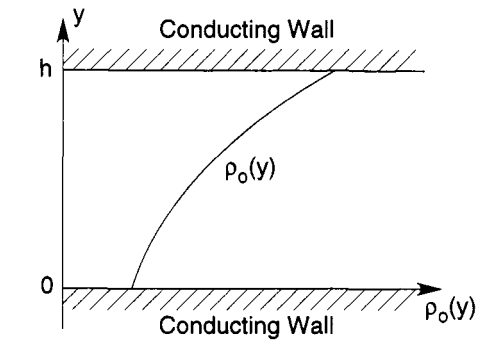

Figure 19.2. The profile of plasma mass density $\rho_0(y)$ between conducting walls at $y = 0$, h.

The equilibrium situation has $\mathbf{u}_0 = 0$, and p_0, B_0 and ρ_0 functions of y alone. (Here, the subscript '0' denotes an *equilibrium* quantity.) The pressure-balance condition (Chapter 9), including an additional gravitational force, requires that

$$\frac{\partial}{\partial y}\left(p_0 + \frac{B_0^2}{2\mu_0}\right) + \rho_0 g = 0 \tag{19.2}$$

where g is the magnitude of the gravitational acceleration, i.e. $\mathbf{g} = -g\hat{\mathbf{y}}$. From equation (19.2) and by referring to Figures 19.1 and 19.2, we see that the field strength B_0 must be larger in the 'vacuum' region than in the 'plasma' region, both to support the pressure gradient and to balance the gravitational force, implying that $\partial B_0/\partial y < 0$.

We now embark on a linearized small-amplitude stability analysis of this equilibrium. We suppose that the plasma equilibrium is perturbed in some way, so that all quantities (densities, fields, etc.) differ from their equilibrium values by infinitesimal but non-zero amounts. However, we neglect all products of two or more infinitesimal quantities (linearized analysis). Unlike the equilibrium, the perturbations will vary in time. For linearized equations, the three types of time dependence that can arise for a perturbation quantity ψ can all be expressed in the form $\psi \propto \exp(-i\omega t)$, where a real value of the 'frequency' ω will correspond to an oscillating perturbation, an ω value with a positive imaginary part will

correspond to an exponentially growing perturbation (instability), and an ω value with a negative imaginary part will correspond to a damped perturbation.

For an equilibrium that is spatially uniform in some direction, say the x direction, the spatial eigenfunctions of the linearized system of equations will be sinusoidal in x, i.e. they can be expressed in the form $\psi \propto \exp(ikx)$, where k is the wave-number. If the equilibrium is not only uniform but also infinitely long in the x direction, then all real k values are allowed. Thus, stability problems of this kind are generally analyzed by assuming that perturbation quantities vary, for example, like

$$\psi \propto \hat{\psi}(y)\exp(ikx - i\omega t) \tag{19.3}$$

for some complex ω to be determined. If ω turns out to be imaginary (with a positive imaginary part), the system can be said to be 'unstable'.

Since the particular equilibrium under investigation here is uniform and infinitely long in the x direction, we adopt precisely the above form for all perturbation quantities. Moreover, the dynamics of the Rayleigh–Taylor instability is *purely two-dimensional*: there is no variation at all (equilibrium or perturbations) *along* the magnetic field (z direction). Thus, while a more general perturbation would have the form

$$\psi \propto \hat{\psi}(y)\exp(ik_x x + ik_z z - i\omega t) \tag{19.4}$$

we may take $k_z = 0$ in this particular problem. In all cases, the eigenfunctions $\hat{\psi}(y)$ are to be determined by finding solutions that correspond to normal modes, i.e. perturbations that have a single (complex) frequency ω.

Accordingly, we are to investigate perturbations of the equilibrium shown in Figures 19.1 and 19.2, in which all quantities (densities, pressures, fields and so on) are of the form

$$f = f_0(y) + f_1(y)\exp(ikx - i\omega t) \tag{19.5}$$

where the subscript '1' denotes small perturbations, and where we have suppressed the suffix in k_x, writing simply k for the x component of the **k**-vector. Such solutions represent wave-like perturbations of the plasma–vacuum interface, as illustrated in Figure 19.3. If the frequency ω is real, the wave-like perturbation travels in the x direction. The wave-like perturbation is created by the periodic upward and downward (i.e. in the y direction) motion of plasma elements: the plasma elements themselves do not need to move significantly in the x direction. (The situation is exactly analogous to propagating water waves, which are caused mainly by the upward and downward motion of the water, rather than by any lateral motion of the water, so long as the wavelength is short compared with the water depth.) If the ω value is purely imaginary, the wave-like perturbation grows in amplitude, but the wave pattern does not move in the x direction.

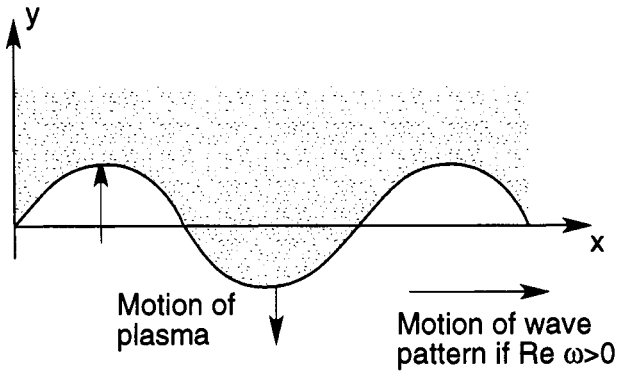

Figure 19.3. A wave-like perturbation of the plasma–vacuum interface shown in Figure 19.1.

An important simplification results from noting that, for this type of perturbation, the field lines *remain straight* even in the perturbed state. This is intuitively obvious from our general result that plasma elements initially on some given field line remain on the same field line in any 'ideal' (i.e. infinite-conductivity) magnetohydrodynamic motion. For, if plasma elements simply move up or down in a wave-like pattern that extends uniformly to infinity in the z direction, then there is no way in which the field lines can become bent. The same result may be obtained formally by examining each component of the linearized version of the usual combination of Faraday's law and the ideal MHD Ohm's law, namely

$$\frac{\partial \mathbf{B}_1}{\partial t} = \nabla \times (\mathbf{u}_1 \times \mathbf{B}_0) = (\mathbf{B}_0 \cdot \nabla)\mathbf{u}_1 - (\mathbf{u}_1 \cdot \nabla)\mathbf{B}_0 - \mathbf{B}_0(\nabla \cdot \mathbf{u}_1) \qquad (19.6)$$

where we have dropped a term in $\nabla \cdot \mathbf{B}_0$ from the right-hand side. (Note that, in this case, the plasma velocity $\mathbf{u}_0$ is zero in the equilibrium and has *only* a perturbed value, denoted by $\mathbf{u}_1$.) If we examine the x and y components of equation (19.6) we see that, in each case, all three terms on the right-hand side vanish identically. The first term on the right-hand side always vanishes since $\mathbf{B}_0 \cdot \nabla = B_0(\partial/\partial z) = 0$. The x and y components of the second and third terms vanish because $\mathbf{B}_0$ has only a z component. Thus, no components B_x or B_y can arise, and the field lines remain straight.

For straight field lines, the linearized perturbed fluid equation of motion is simply

$$\rho_0 \frac{\partial \mathbf{u}_1}{\partial t} = \rho_1 \mathbf{g} - \nabla \left(p_1 + \frac{B_0 B_{z1}}{\mu_0} \right). \qquad (19.7)$$

Here we have linearized the magnetic-pressure perturbation, i.e. $(B^2)_1 = 2B_0 B_{z1}$.

Both x and y components of this linearized equation of motion provide useful information. However, since we do not at present have much additional information about either p_1 or B_{z1}, it is convenient to eliminate these two quantities by taking the z component of the curl of the equation of motion, i.e. operating on both sides of equation (19.7) with the operator $\hat{\mathbf{z}} \cdot \nabla \times$. This corresponds to taking $\partial/\partial x$ of the y component and subtracting $\partial/\partial y$ of the x component, eliminating the entire gradient term on the right-hand side, since the curl of a gradient vanishes. What remains is

$$-\mathrm{i}\omega\left(\mathrm{i}k\rho_0 u_y - \frac{\partial}{\partial y}(\rho_0 u_x)\right) = -\mathrm{i}k\rho_1 g \tag{19.8}$$

where we have dropped the subscript '1' from the velocity components.

Let us, for the moment, suppose that the plasma motion is incompressible, i.e.

$$\begin{aligned} 0 = \nabla \cdot \mathbf{u}_1 &= \mathrm{i}ku_x + \frac{\partial u_y}{\partial y} \\ u_x &= \frac{\mathrm{i}}{k}\frac{\partial u_y}{\partial y}. \end{aligned} \tag{19.9}$$

(This assumption replaces the adoption of an adiabatic or isothermal equation of state. Its validity is only approximate, but will be verified later after we have completed our calculation.) With this assumption, the density perturbation can be obtained from the continuity equation, as follows:

$$\frac{\partial \rho_1}{\partial t} + \mathbf{u}_1 \cdot \nabla \rho_0 = 0 \tag{19.10}$$

giving

$$\begin{aligned} -\mathrm{i}\omega\rho_1 &= -u_y \frac{\partial \rho_0}{\partial y} = -\frac{\rho_0 u_y}{s} \\ \rho_1 &= \frac{\rho_0 u_y}{\mathrm{i}\omega s} \end{aligned} \tag{19.11}$$

the latter for our particular form of $\rho_0(y)$. Substituting from the continuity equation (19.11) for ρ_1, and the incompressibility relation (19.9) for u_x into the equation of motion (19.8), we obtain

$$\frac{1}{\rho_0}\frac{\partial}{\partial y}\left(\rho_0 \frac{\partial u_y}{\partial y}\right) - k^2\left(1 + \frac{g}{s\omega^2}\right)u_y = 0. \tag{19.12}$$

This is a second-order differential equation for a single spatial variable, $u_y(y)$, as a function of an unknown scalar quantity ω, which can be solved

once the appropriate boundary conditions are specified. Since the differential equation is homogeneous, it will be possible to satisfy *two* boundary conditions only for some discrete set of 'eigenvalues', which will determine the allowed set of values for ω. As we have already indicated in Figure 19.2, we suppose that the plasma is bounded above and below by conducting walls, taken to be at $y = 0$ and $y = h$. (A conducting wall cannot have any **E** field parallel to its surface, and thus the perpendicular component of the plasma velocity must also vanish. In this sense, the wall is a 'rigid' boundary in regard to fluid motion.) Thus, the boundary conditions are

$$u_y = 0 \qquad \text{at} \qquad y = 0, h. \tag{19.13}$$

By design, we chose a form for $\rho_0(y)$ for which the differential equation can be solved analytically. By using an integrating factor $\exp(-y/2s)$, discrete solutions ('eigenfunctions') of equation (19.12) may be found of the form

$$u_y(y) = \sin\left(\frac{n\pi y}{h}\right)\exp\left(-\frac{y}{2s}\right) \tag{19.14}$$

for all integer values of n. The 'eigenvalues', which for equation (19.12) will give the allowed values for the quantity $g/(s\omega^2)$, are given by the relation

$$k^2\left(1+\frac{g}{s\omega^2}\right) = -\frac{1}{4s^2} - \frac{n^2\pi^2}{h^2}. \tag{19.15}$$

Problem 19.1: Verify equation (19.15) by direct substitution of equation (19.14) into equation (19.12).

For the case where g and s are both positive, as they are for the configuration illustrated by Figures 19.1 and 19.2, we see immediately that there are no solutions unless ω^2 is negative, corresponding to ω being pure imaginary. Solving for ω, we obtain

$$\omega = \pm \mathrm{i}\left(\frac{g}{s}\frac{h^2k^2}{n^2\pi^2 + h^2k^2 + h^2/4s^2}\right)^{1/2}. \tag{19.16}$$

The solution for ω with a positive imaginary part represents an *exponentially growing perturbation*, i.e. an *instability*. The solution with a negative imaginary part represents a decaying perturbation that is of no interest.

The lowest mode that satisfies our boundary conditions has $n = 1$. This is the 'longest wavelength' mode in the y direction and is more rapidly growing

than modes with $n > 1$. The fastest growing modes tend to be those with the shortest wavelengths in the x direction, however, i.e. large k values. Indeed, for all modes with wavelengths in the x direction that are shorter than both the density scale-length s and the geometric height of the plasma h, i.e. those with $hk \gg \pi$ and $ks \gg 1$, the growth rate γ (the imaginary part of ω for the growing $n = 1$ mode) is given by

$$\gamma = (g/s)^{1/2}. \tag{19.17}$$

The 'growth time' $\gamma^{-1} = (s/g)^{1/2}$ is just the time for 'free fall' over a distance s due to the gravitational acceleration g.

If the sign of either g or s is reversed, corresponding to the case of the plasma density increasing in the direction of the gravitational force $\mathbf{g}$, the solutions for ω are all real. This case is *stable*, and the eigenmodes are propagating wave-like disturbances.

19.2 ROLE OF INCOMPRESSIBILITY IN THE RAYLEIGH–TAYLOR INSTABILITY

In the discussion of the Rayleigh–Taylor instability given in the previous Section, we assumed the plasma flow to be incompressible, i.e.

$$\nabla \cdot \mathbf{u} = 0. \tag{19.18}$$

We will now verify the validity of this approximation.

Physically, incompressibility is a good approximation because the potential energy of the plasma in the gravitational field is usually insufficient to provide either the increase in thermal energy that occurs in compression of the plasma, or the increase in magnetic-field energy that occurs as the magnetic field is (necessarily) compressed along with the plasma. Let us consider this latter effect, since it is the more important in a plasma with a low β value ($p \ll B^2/2\mu_0$).

The geometrical configuration is the same as in the previous Section, as shown in Figure 19.1. As we saw before, the magnetic field lines remain straight, and no B_x or B_y components arise. The perturbation in the B_z component may be obtained by combining Faraday's and Ohm's laws in the usual manner:

$$\frac{\partial \mathbf{B}_1}{\partial t} = \nabla \times (\mathbf{u}_1 \times \mathbf{B}_0) = (\mathbf{B}_0 \cdot \nabla)\mathbf{u}_1 - (\mathbf{u}_1 \cdot \nabla)\mathbf{B}_0 - \mathbf{B}_0(\nabla \cdot \mathbf{u}_1). \tag{19.19}$$

Taking the z component gives

$$\frac{\partial B_{1z}}{\partial t} + (\mathbf{u}_1 \cdot \nabla)B_0 = -\mathrm{i}\omega B_{z1} + u_y \frac{\partial B_0}{\partial y} = -B_0(\nabla \cdot \mathbf{u}_1). \tag{19.20}$$

This simply tells us that the magnetic field is convected and compressed along with the plasma. Henceforth, we again drop the subscript '1' from the velocity components.

To relate the energy needed to produce this amount of compression to the potential energy that is available, we consider one of the individual components of the equation of motion, say the x component:

$$\rho_0 \frac{\partial u_x}{\partial t} = -\frac{\partial}{\partial x}\left(p_1 + \frac{B_0 B_{z1}}{\mu_0}\right). \tag{19.21}$$

This equation balances the forces arising from compression of the plasma and magnetic field with the accelerating or decelerating flow that drives this compression. Recall that, in the previous Section, we conveniently eliminated both p_1 and B_{z1} by taking $\partial/\partial y$ of this x component of the equation of motion and subtracting $\partial/\partial x$ of the y component. The assumption of incompressibility allowed us to use this trick to avoid treating the effects of p_1 and B_{z1} directly. Here, we must retain these two quantities and use equation (19.21) in the form

$$-\mathrm{i}\omega\rho_0 u_x \approx -\mathrm{i}k(p_1 + B_0 B_{z1}/\mu_0). \tag{19.22}$$

We now use the adiabatic gas law to find the perturbation in the pressure, p_1. From $\mathrm{d}p/\mathrm{d}t = (\gamma p/\rho)\mathrm{d}\rho/\mathrm{d}t$, we obtain

$$\frac{\partial p_1}{\partial t} + (\mathbf{u}_1 \cdot \nabla)p_0 = -\mathrm{i}\omega p_1 + u_y \frac{\partial p_0}{\partial y} = -\gamma p_0(\nabla \cdot \mathbf{u}_1). \tag{19.23}$$

We may now substitute equation (19.20) for B_{z1} and equation (19.23) for p_1 into equation (19.22). After considerable rearranging of terms, equation (19.22) then becomes:

$$\mathrm{i}ku_x = \frac{k^2}{\omega^2}\left(\frac{\gamma p_0}{\rho_0} + \frac{B_0^2}{\rho_0\mu_0}\right)\nabla \cdot \mathbf{u}_1 + \frac{k^2 u_y}{\omega^2 \rho_0}\frac{\partial}{\partial y}\left(p_0 + \frac{B_0^2}{2\mu_0}\right). \tag{19.24}$$

We may simplify the second term on the right-hand side of equation (19.24) by using the equilibrium relation (19.2). For the eigenfunctions and eigenvalues described by equations (19.14) and (19.16), respectively, it will then be seen that the second term on the right-hand side of equation (19.24) has the same order-of-magnitude as the term on the left-hand side. However, the coefficient of the first term on the right-hand side of equation (19.24) (for $p_0 \ll B_0^2/\mu_0$) is approximately $k^2 B_0^2/\omega^2\rho_0\mu_0 = k^2 v_A^2/\omega^2$. Thus, from equation (19.24), we obtain the order-of-magnitude relationship:

$$\frac{\nabla \cdot \mathbf{u}_1}{\mathrm{i}ku_x} \sim \frac{\omega^2}{k^2 v_A^2} \tag{19.25}$$

where $v_A = B_0/(\rho_0\mu_0)^{1/2}$ is the Alfvén speed. Noting that

$$\nabla \cdot \mathbf{u}_1 = \mathrm{i}ku_x + \frac{\partial u_y}{\partial y}$$

we see that equation (19.25) expresses the *neglected* quantity ($\nabla \cdot \mathbf{u}_1$) as a fraction of a *retained* quantity, in this case iku_x. This fraction clearly measures how good the incompressibility approximation is. If the fraction is very small, the two terms in $\nabla \cdot \mathbf{u}_1$ must almost cancel, i.e. to a good approximation we may assume that $\nabla \cdot \mathbf{u}_1 = 0$. Thus, the incompressibility approximation is valid whenever

$$|\omega^2| \ll k^2 v_A^2. \tag{19.26}$$

Conversely, a flow with finite compression, i.e. in which $\nabla \cdot \mathbf{u}_1$ is as large as either of its constituent parts, e.g. iku_x, would result in a higher-frequency wave, whose phase velocity perpendicular to the magnetic field would be comparable to the Alfvén speed. In the terminology of Chapter 18, this would be the 'compressional' Alfvén wave, or the 'magnetosonic' wave.

In the case of an instability, the magnitude of the growth rate will be a measure of the amount of potential energy available to drive the compression. For the Rayleigh–Taylor instability, which has a growth rate (see equation (19.16)) given by

$$|\omega^2| = |\gamma^2| = \frac{g}{s} \frac{h^2 k^2}{n^2\pi^2 + h^2 k^2 + h^2/4s^2}$$

the incompressibility condition, equation (19.26), is valid whenever

$$gs \ll v_A^2 \left(\frac{n^2\pi^2 s^2}{h^2} + k^2 s^2 + \frac{1}{4} \right). \tag{19.27}$$

Equation (19.27) is least easily satisfied for the longest wavelengths, i.e. the smallest values of n and ks. Even then, it is satisfied whenever

$$\rho g s \ll \rho v_A^2 \approx B^2/\mu_0 \tag{19.28}$$

i.e. whenever the gravitational potential energy is much less than the magnetic field energy. For shorter wavelengths, the approximation is even better.

This agrees with our initial intuitive observation: incompressibility should be a very good approximation whenever the potential energy that is available from the gravitational field is inadequate to provide the energy needed for compression of the magnetic field.

It must be emphasized that the approximate incompressibility of the plasma is the consequence, for the particularly simple geometry under consideration here, of the plasma's inability to compress the magnetic field due to the smallness of the available gravitational potential energy. Equivalently, the compressional Alfvén wave, or magnetosonic wave, cannot be excited: the instability arises, in effect, in the 'shear' Alfvén wave in the special case where $k_\parallel = 0$. For this wave, to minimize the effect of the magnetosonic branch, the perturbation

quantities B_{z1} and p_1 are relatively small (although non-zero) and are related to each other through the equation of motion, e.g. equation (19.21). They are also both described in terms of a combination of convection and a small amount of compression, as given in equations (19.20) and (19.23), respectively. Equation (19.20) expresses the conservation of magnetic flux in our assumed perfectly conducting plasma which is *exact*, in contrast to incompressibility, which is only *approximate*. We will see below that there are other geometries in which the Rayleigh–Taylor instability can be *driven* by expansion (i.e. negative compression) of the plasma. In these cases, the expansion is just that necessary to conserve magnetic flux in a plasma that is convecting into a region of reduced magnetic field. There is still little expansion/compression of the *magnetic field*, i.e. still little coupling to the magnetosonic wave.

19.3 PHYSICAL MECHANISMS OF THE RAYLEIGH–TAYLOR INSTABILITY

As a complement to the fluid picture developed above, the physical mechanism at work in the Rayleigh–Taylor instability can also be understood in terms of the *gravitational drifts* of ions and electrons.

From Chapter 2, we recall that an external force **F** (such as a gravitational force $\mathbf{F} = M\mathbf{g}$) perpendicular to a magnetic field **B** causes a charged particle (in particular, an ion with charge $+e$) to drift with a velocity

$$\mathbf{v}_d = \frac{\mathbf{F} \times \mathbf{B}}{eB^2} = \frac{M\mathbf{g} \times \mathbf{B}}{eB^2}. \tag{19.29}$$

In our case (see Figure 19.1), this gravitational drift is in the negative-x direction, and has the magnitude $v_d = Mg/eB$. There is also an electron drift in the opposite direction, but this is much smaller because of the smaller electron mass.

Suppose a small wave-like ripple should develop on a 'plasma–vacuum interface', as shown in Figure 19.3. The gravitational drift of ions on the plasma side of the interface will cause positive charge to build up on one side of the ripple, as illustrated in Figure 19.4; the depletion of ions causes a negative charge to build up on the other side of the ripple. Due to this separation of charges, a small electric field $\mathbf{E}_1$ develops, and this electric field changes sign going from crest to trough of the perturbation, again as shown in Figure 19.4. It is apparent that the resulting $\mathbf{E}_1 \times \mathbf{B}_0$ drift is always upward in those regions where the interface has already moved upward, and downward in those regions where the interface has already moved downward. Thus the initial ripple grows larger, as a result of $\mathbf{E} \times \mathbf{B}$ drifts that are phased so as to amplify the initial perturbation.

The Rayleigh–Taylor instability can also be understood from an energy viewpoint, i.e. in terms of the lowering of the plasma's potential energy in the

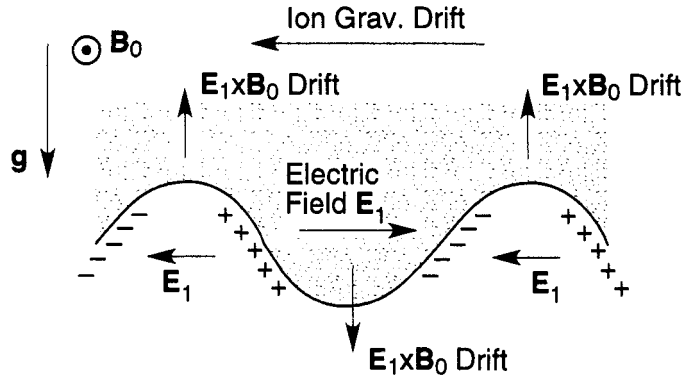

Figure 19.4. The mechanism of the Rayleigh–Taylor instability. The ion gravitational drift leads to charge separation on the plasma–vacuum interface, producing electric fields and $\mathbf{E} \times \mathbf{B}$ drifts that increase the amplitude of the perturbation.

gravitational field due to the growth of the instability. However, the change in potential energy is *second order* in the amplitude of the perturbations. For the simple case illustrated in Figure 19.3, this second-order change in the gravitational potential energy can be calculated explicitly. Suppose the plasma shown in Figure 19.3 has uniform density ρ and extends from the plasma–vacuum interface at $y = 0$ to some fixed upper boundary at $y = h$. Before the onset of the wave-like perturbation of the plasma's lower surface, the gravitational potential energy is simply

$$\int \rho g y \mathrm{d}x\mathrm{d}y = \rho g L h^2/2$$

where the integral over y has been taken from $y = 0$ to $y = h$ and the integral over x has been taken over some length L. Now add a sinusoidal perturbation of the plasma's lower surface, which may be assumed to take the shape $y = \xi \sin kx$, as shown in Figure 19.3. This perturbation satisfies the incompressibility constraint since the area of the plasma in the (x, y) plane is unchanged (see Figure 19.3). The plasma fills the region above this deformed lower boundary, still with uniform mass density, ρ. The gravitational potential energy is still $\int \rho g y \mathrm{d}x\mathrm{d}y$, but the integral over y must now be taken from $y = \xi \sin kx$ to $y = h$ and the integral over x may most conveniently be taken over the length of a full period, $L = 2\pi/k$; the gravitational potential energy becomes

$$\rho g \int (h^2 - \xi^2 \sin^2 kx)\mathrm{d}x/2 = \rho g L(h^2 - \xi^2/2)/2.$$

Thus the gravitational potential energy is *lowered* by an amount $\rho g L \xi^2/4$ (second order in the perturbation amplitude ξ) by the onset of the perturbation.

When potential energy can be lowered by such a perturbation, so that the energy released can go into kinetic energy of plasma motion, this can provide the energy necessary to drive an instability.

19.4 FLUTE INSTABILITY DUE TO FIELD CURVATURE

Real gravitational forces are generally totally negligible in laboratory plasma physics: plasmas are much too rarefied for gravity to compete with the strong pressure gradients and magnetic forces. The importance of the Rayleigh–Taylor instability lies in the close analogy between *gravitational drifts* and the ∇B and *curvature drifts* that arise in non-uniform magnetic fields.

In Chapter 3, we obtained the following expression for the combined ∇B and curvature drifts of an ion with charge e in a *vacuum* magnetic field (which should provide an adequate approximation to the actual magnetic field in a low-β plasma without strong field-aligned currents):

$$\mathbf{v}_d = \frac{M}{e}\left(\frac{v_\perp^2}{2} + v_\parallel^2\right)\frac{\mathbf{R}_c \times \mathbf{B}}{R_c^2 B^2} \tag{19.30}$$

where $\mathbf{R}_c$ is the vector radius-of-curvature (a vector drawn from the local center-of-curvature to the field line, intersecting the field line normally and pointing away from the center-of-curvature). By comparing equation (19.30) with the expression for the gravitational drift given in equation (19.29), we see that the gravitational drift provides a good model for the drifts in a curved magnetic field, provided the vectors $\mathbf{g}$ and $\mathbf{R}_c$ are in the same direction, and the magnitude of g is defined by

$$g = \left(\frac{v_\perp^2}{2} + v_\parallel^2\right)\frac{1}{R_c}. \tag{19.31}$$

If we average over a thermal distribution of particle velocities $v_\perp$ and $v_\parallel$, we can write $\langle v_\parallel^2\rangle = \langle v_\perp^2/2\rangle = T/M = p/\rho$, which shows that the magnitude of g should be related to the ion pressure p of a plasma in a curved magnetic field by

$$g = \frac{2p}{\rho R_c}. \tag{19.32}$$

Since the thermal velocities of electrons are much larger than those of ions, *both* particle species have comparable curvature and ∇B drifts, whereas the gravitational drift is important only for ions. The effect of this is that the total pressure, ions and electrons, should be used for p in equation (19.32).

Thus a plasma in a curved magnetic field can be viewed as having analogous particle drifts to a plasma in a gravitational field—and therefore a potential for charge build-up and unstable growth of perturbations. Since the Rayleigh–Taylor instability arises whenever the gravitational force is directed away from

the region of maximum plasma density, the corresponding instability of a plasma in a curved field arises whenever the *radius-of-curvature vector is directed away from the region of maximum plasma pressure,* i.e. *whenever the plasma is confined by a magnetic field that is concave towards the plasma.*

The growth rate γ of the instability can be estimated by replacing g by $2p/\rho R_c$ in the expression for γ given in equation (19.17) and by equating the scale-length s to the pressure-gradient scale-length, i.e. $s^{-1} = |\nabla p|/p$. We obtain

$$\gamma \approx (2|\nabla p|/\rho R_c)^{1/2}. \tag{19.33}$$

We reiterate that this instability occurs only if the radius-of-curvature vector is directed away from the region of maximum plasma pressure, i.e. only if $\mathbf{R}_c$ and ∇p are oppositely directed.

This pressure-driven version of the Rayleigh–Taylor instability, which in the next Section we will learn to call the 'flute instability', is rapidly growing. The growth time (i.e. γ^{-1}) can be estimated by noting that $p/\rho \approx C_s^2$, where C_s is the sound speed in the plasma, giving

$$\gamma \sim C_s/(sR_c)^{1/2}. \tag{19.34}$$

Thus, the characteristic growth time is the time it takes a sound wave to traverse a distance that is the geometric mean of the pressure-gradient scale-length and the radius-of-curvature.

Problem 19.2: An annular cylindrical plasma, as shown in Figure 19.5, is *infinitely long* in the z direction. It has a purely azimuthal magnetic field $B_\theta(r)$, produced mainly by the current I in a central conductor at $r = 0$. The plasma pressure $p(r)$ falls to zero on both the inside of the annular cylinder, $r = r_1$, and on the outside, $r = r_2$, peaking somewhere between r_1 and r_2. Describe carefully by means of an illustration why you would expect this plasma to be subject to the Rayleigh–Taylor flute instability. For simplicity, you may suppose that $p \ll B_\theta^2/\mu_0$, so that the field is approximately the vacuum field, $B_\theta \propto r^{-1}$. Indicate in your illustration the particle drifts that give rise to this instability, and show the form that the unstable perturbations will take.

19.5 FLUTE INSTABILITY IN MAGNETIC MIRRORS

One configuration that is obviously susceptible to the pressure-driven version of the Rayleigh–Taylor instability is the *magnetic mirror*, in which a cylindrical plasma with an approximately axial magnetic field is constricted at both ends

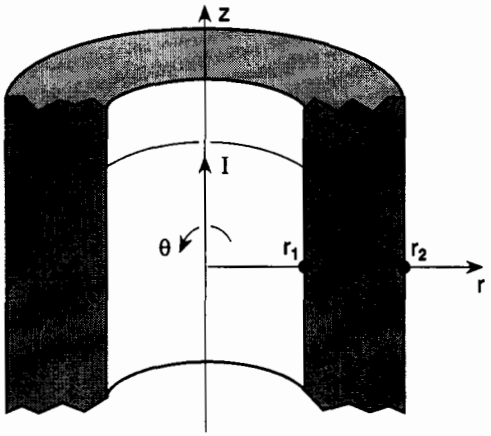

Figure 19.5. Annular cylindrical plasma, infinitely long in the z direction, has a purely azimuthal field $B_\theta(r)$ produced by the current I in a central conductor at $r = 0$. See Problem 19.2.

by regions of higher field strength, as shown in Figure 19.6. In this case, the curvature of the magnetic field is clearly concave toward the plasma in the central region. Approximating the plasma as a long cylinder, in which the pressure is considered to be a function of the radius r, the growth rate of the instability will be given by

$$\gamma \approx \left(-\frac{2p'(r)}{\rho R_c}\right)^{1/2} \tag{19.35}$$

where the prime denotes differentiation with respect to r.

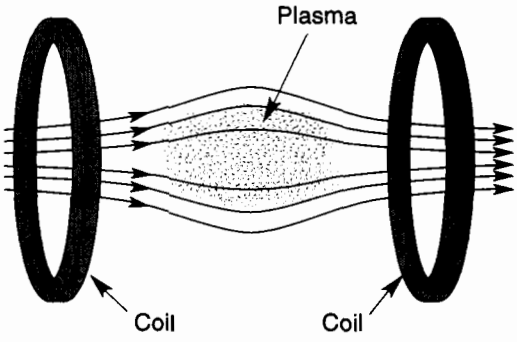

Figure 19.6. Plasma equilibrium in a 'magnetic mirror' configuration. Note that the magnetic field curvature is concave toward the plasma in the central region where the plasma pressure is largest.

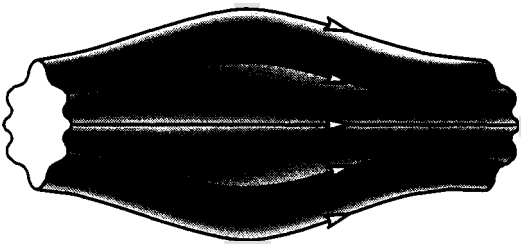

Figure 19.7. Flute-like perturbation of a magnetic-mirror plasma produced by the Rayleigh–Taylor instability.

This Rayleigh–Taylor instability will produce a rippling of the plasma surface in the azimuthal direction, and the ripples will extend uniformly along the length of the cylinder. The form of the perturbation is illustrated in Figure 19.7. The pressure-driven version of the Rayleigh–Taylor instability is called the 'flute instability' because of the resemblance of the perturbed surface of a quasi-cylindrical plasma such as this to a fluted Greek column.

Problem 19.3: Consider a cylindrical plasma with an axial field B_0 that is made flute-unstable by constricting the ends to form a magnetic-mirror configuration. Consider a flute instability with azimuthal mode number m, i.e. a mode in which the perturbations vary as $\exp(im\theta)$. Use the appropriate expression for the growth rate γ to show that the incompressibility approximation is valid whenever $\beta r/R_c \ll m^2$.

The basic energy reason for the flute instability in a curved magnetic field is very similar to the energy reason for the gravitational instability. Just as a fluid supported against gravity can lower its *potential* energy by perturbations that push downward in the direction of $\mathbf{g}$, so the *thermal* energy of a flute-unstable plasma can be lowered by perturbations that push outward in the direction of $\mathbf{R}_c$. That such perturbations produce a net expansion of the plasma, and thus release thermal energy, can be shown explicitly in the case of a low-β mirror-confined plasma, as follows.

We have already seen that there is not enough energy to compress the magnetic field, but in a low-β plasma an even stronger condition applies, namely that the magnetic field is essentially a vacuum field and remains approximately unchanged even when the plasma pushes outward across this field. However, the total magnetic flux contained within the plasma, i.e. the quantity $\int B\mathrm{d}S$ integrated over the plasma cross section, must remain exactly constant, and so the only type of perturbation permitted is that illustrated in Figure 19.7, in which the

surface of the plasma becomes rippled by 'filaments' of plasma moving outward, while compensating 'filaments of vacuum' move inward so as to conserve the total magnetic flux. The perturbations must be 'flutes', i.e. uniform along the entire length of the plasma, so as to avoid 'bending' the magnetic field, which would require additional energy. To the extent that special effects occur at the ends of the magnetic mirror which limit the allowed perturbations in this area (e.g. conducting plates could be placed at the ends of the mirror), then these effects will have a stabilizing influence; this topic is beyond the scope of the present discussion. Such effects are required, however, to explain the stability of the Earth's magnetosphere.

If the strength of the magnetic field decreases in the radially outward direction (as it does in the central region of the magnetic mirror, where the field gradient arises because the field is concave towards the plasma), the rippling perturbation of the plasma surface that conserves magnetic flux must result in a small (second-order) increase in the area of the plasma cross section. This is because the filaments of plasma which move outward are moving into a region of lower field, and so these cross section areas must increase, relative to the cross sectional areas of the 'vacuum filaments' of equal magnetic flux which move inward into a region of higher field. This increase in net cross sectional area results in a corresponding increase in plasma volume. The concave (towards the plasma) curvature of the magnetic field results in another (second-order) increase in the plasma volume, because the plasma filaments moving outward are lengthened slightly, relative to the vacuum filaments moving inward, which are shortened. For vacuum magnetic fields the gradient and curvature effects are always additive (corresponding to the ∇B and curvature drifts always being in the same direction). The increase in volume, due both to increased cross sectional area and increased field-line length, corresponds to *expansion* of the plasma and a lowering of its thermal energy, thereby making energy available for the unstable perturbation.

From a single-particle perspective, the drop in perpendicular and parallel particle kinetic energy associated with moving to lower B and higher R_c is invested in $j \cdot E$ work, as discussed in Section 3.5. This $j \cdot E$ work *drives* the instability to higher amplitudes.

Closer examination of the mirror field configuration, however, shows that there are regions of *favorable* curvature (convex toward the plasma) near the ends, in addition to the main region of unfavorable (concave) curvature at the center. In general, however, in axisymmetric mirror configurations the unfavorable curvature is dominant. However, *non-axisymmetric* mirror configurations have been designed for fusion applications in which current-carrying rods, first used by M C Ioffe (see Y B Gott *et al* 1962 *Nuclear Fusion Suppl.* p 1042), are placed outside the plasma, parallel to its axis, so as to create a B_θ field with favorable curvature, i.e. convex toward the plasma. In such

cases, the combined curvature can be favorable everywhere; indeed the plasma is located in the region of an absolute minimum in the strength of the vacuum magnetic field.

The correct weighting of the favorable and unfavorable regions in a 'simple mirror' can be derived as follows. Take cylindrical coordinates (r, θ, z), with z along the axis of the mirror field. Overall stability will be determined by the average net angular drift of particles over their complete orbits along the mirror field from one end to the other. If the sign of this average net angular drift corresponds to field curvature that is concave toward the plasma, there will be a build-up of charges on the edges of the flutes which will give rise to azimuthal **E** fields that produce unstable growth in the amplitude of the flute-like perturbations. In the simple mirror geometry, the ∇B and curvature drifts are entirely azimuthal in direction, so that the angular drift speed of an individual particle is given by

$$r\frac{\mathrm{d}\theta}{\mathrm{d}t} = \frac{m}{eR_cB}\left(v_\parallel^2 + \frac{v_\perp^2}{2}\right). \tag{19.36}$$

In one complete orbit along the mirror field, the net angular drift of this particle is given by

$$\Delta\theta = \frac{m}{e}\int \frac{(v_\parallel^2 + v_\perp^2/2)\mathrm{d}\ell}{rR_cBv_\parallel} \tag{19.37}$$

where we have written $\mathrm{d}t = \mathrm{d}\ell/v_\parallel$, where ℓ is a length coordinate along the field line. The particle's velocity components, $v_\parallel$ and $v_\perp$, change as the particle moves along the field line, i.e. are functions of ℓ in the integral in equation (19.37), and these changes will be such as to conserve the particle energy $W = mv^2/2$ and the magnetic moment $\mu = mv_\perp^2/2B$.

To obtain the net angular drift averaged over all particles in a filamentary 'flux tube', i.e. a thin tube which follows the magnetic field and contains a given number of magnetic field lines, it is simplest to return to equation (19.36) and average $\mathrm{d}\theta/\mathrm{d}t$ over the velocity-space distribution function, f, and over a flux tube containing a small amount of magnetic flux, $\Delta\Phi$. At any point along this flux tube, its cross sectional area is given by $\Delta A = \Delta\Phi/B$. The total number of particles contained in the flux tube is $\Delta N = \int n\mathrm{d}A\mathrm{d}\ell$. Dividing equation (19.36) by r, multiplying by the distribution function, f, and integrating both over velocity space and over the volume of the flux tube, we obtain

$$\Delta N\left\langle\frac{\mathrm{d}\theta}{\mathrm{d}t}\right\rangle = \frac{m}{e}\Delta\Phi\int \frac{v_\parallel^2 + v_\perp^2/2}{rR_cB^2} f\mathrm{d}^3v\mathrm{d}\ell \tag{19.38}$$

Equation (19.38) gives the average rate at which the entire population of particles of a given species in a given flux tube drifts azimuthally in θ to a neighboring flux tube. The direction of the drift is opposite for electrons and ions, as expected

for gradient and curvature drifts, so the contributions from both species to the drift of *charge* are additive. Carrying out the local velocity-space integrals in equation (19.38) and omitting various positive multiplicative factors, we find that the average angular drift of charge is given by

$$\left\langle \frac{\mathrm{d}\theta}{\mathrm{d}t} \right\rangle \propto \int \frac{p_{\parallel} + p_{\perp}}{r R_{\mathrm{c}} B^2} \mathrm{d}\ell. \tag{19.39}$$

Adopting the convention that field lines that are concave toward the plasma have positive radii-of-curvature, while convex field lines have negative radii-of-curvature, the condition for flute instability is that the integral in equation (19.39) be positive, i.e. that the regions of positive R_{c} outweigh the regions of negative R_{c}. The point of inflection, which separates these two regions, has an infinite R_{c} and contributes negligibly to the integral in equation (19.39).

Unfortunately, the weighting due to $1/rB^2$ in the integrand of equation (19.39) is unfavorable, in that B is smallest where R_{c} is positive. In general, therefore, the simple mirror is unstable to flutes.

The flute instability in magnetic mirrors was analyzed first by M N Rosenbluth and C L Longmire (1957 *Ann. Phys.* **1** 120).

19.6 FLUTE INSTABILITY IN CLOSED FIELD LINE CONFIGURATIONS*

An even simpler stability criterion can be obtained for the case where the plasma pressure is isotropic, i.e. $p_{\parallel} = p_{\perp} = p$. In this case, the condition for equilibrium demands that the pressure be uniform along the field, i.e. $\mathbf{B} \cdot \nabla p = 0$. For a mirror-confined plasma, this condition can never be satisfied, or else the plasma would extend infinitely far along the field lines. However, it is possible to create certain 'closed field line' configurations in which each field line closes on itself, so that the plasma pressure can be exactly constant along field lines. An example of such a configuration is the 'toroidal quadrupole' shown in Figure 19.8. Here the plasma entirely surrounds the two coils that produce the magnetic field. (In a practical situation, the coils must either by supported and electrically fed by leads that pass through the plasma, or they must be superconducting and supported magnetically for the duration of the plasma pulse.) From Figure 19.8, it may be seen that some of the plasma lies on field lines that encircle only one coil, whereas the rest of the plasma lies on field lines that pass around both coils. On the inner sides of the plasma which face each single coil, the curvature of the magnetic field is convex toward the plasma, and this interface is stable to flutes. On the outer side of the plasma there are regions of both concave and convex curvature, and so the stability of this interface depends on the appropriate averaging of the favorable and unfavorable contributions, expressed in the form

of a criterion that we will now derive. We will do this for isotropic pressure, and we will assume that the plasma (as in the simple mirror) is axisymmetric, i.e. that the configuration is symmetric to rotation in θ about the z axis in Figure 19.8. In such cases, the pressure can be brought outside the integral in equation (19.39), which then becomes

$$\left\langle \frac{\mathrm{d}\theta}{\mathrm{d}t} \right\rangle \propto \oint \frac{\mathrm{d}\ell}{r R_c B^2} \tag{19.40}$$

with instability corresponding to the case where this integral is positive. (The integral is to be taken along the entire closed field line.)

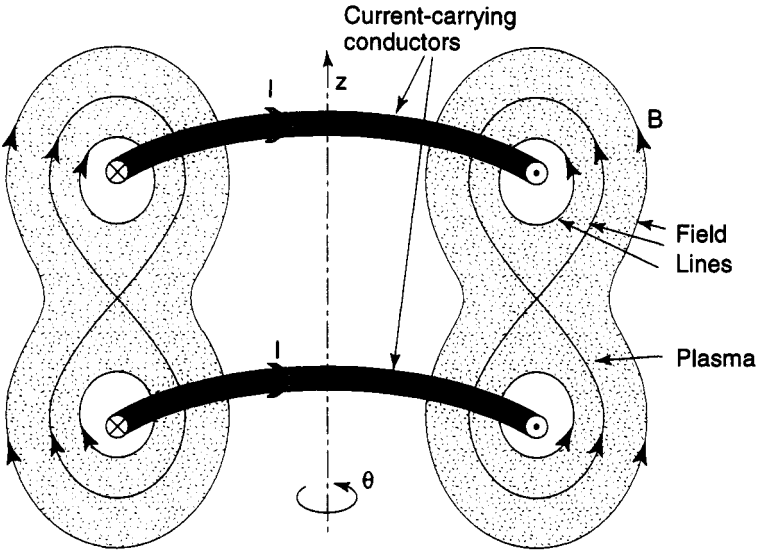

Figure 19.8. The toroidal quadrupole configuration. The plasma entirely surrounds the two current-carrying conductors that produce the magnetic field shown. The configuration is axisymmetric, i.e. symmetric to rotation in θ about the z axis.

In order to derive an even simpler stability criterion, consider two neighboring field lines in the same azimuthal plane (i.e. same θ value) of an axisymmetric configuration. Examine two infinitesimal elements of these neighboring field lines bounded by the same two radius-of-curvature vectors, as shown in Figure 19.9. The field strengths on these two elements are denoted B and $B + \delta B$ and the (infinitesimal) lengths of the elements are denoted $\mathrm{d}\ell$ and $\mathrm{d}\ell + \delta(\mathrm{d}\ell)$. For a vacuum magnetic field, we can use Stokes' theorem to show that

$$\oint \mathbf{B} \cdot \mathrm{d}\boldsymbol{\ell} = \int (\nabla \times \mathbf{B}) \cdot \mathrm{d}\mathbf{S} = 0 \tag{19.41}$$

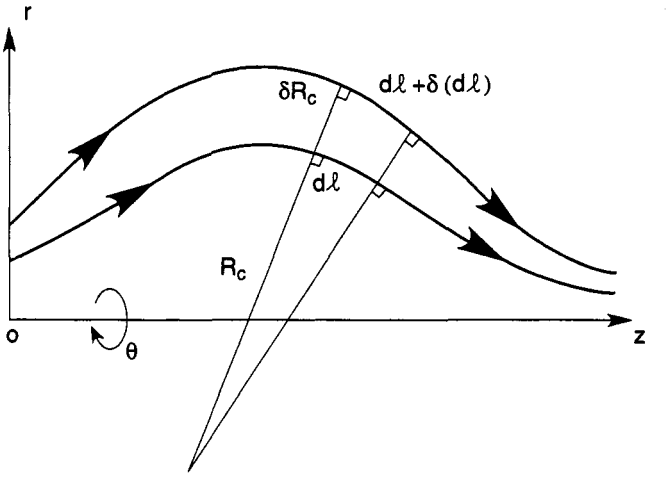

Figure 19.9. Two neighboring field lines in a mirror-like configuration with local radii-of-curvature R_c and $R_c + \delta R_c$. The configuration is axisymmetric, i.e. symmetric to rotation in θ about the z axis.

which, when applied to the infinitesimal closed contour shown in Figure 19.9, tells us that

$$B\mathrm{d}\ell = (B + \delta B)[\mathrm{d}\ell + \delta(\mathrm{d}\ell)] \tag{19.42}$$

that is,

$$\frac{\delta B}{B} = -\frac{\delta(\mathrm{d}\ell)}{\mathrm{d}\ell} = -\frac{\delta R_c}{R_c}. \tag{19.43}$$

Here, in the final step, we have used simple geometry to relate $\delta(\mathrm{d}\ell)$ to the perpendicular distance between the two field lines, δR_c. Since we want to apply equation (19.43) at all points along the two magnetic field lines, it is more convenient to define their separation not by the geometrical distance between them, δR_c, which varies along the field line, but by the magnetic flux between them, which is the same at all points along the field line. A convenient measure of this is the magnetic flux passing through an annular band obtained by rotating the element δR_c shown in Figure 19.9 by one revolution in θ about the axis. Specifically, this magnetic flux is

$$\delta\Phi = 2\pi r B \delta R_c \tag{19.44}$$

so that

$$\frac{\delta B}{B} = -\frac{\delta\Phi}{2\pi r R_c B}. \tag{19.45}$$

We can now write equation (19.40) as

$$\left\langle \frac{d\theta}{dt} \right\rangle \propto -\frac{1}{\delta\Phi} \oint \frac{\delta B}{B^2} d\ell \tag{19.46}$$

(omitting the factor 2π). Let us now consider the quantity $\oint d\ell/B$ and its variation between neighboring field lines, such as those shown in Figure 19.9. We have

$$\delta \oint \frac{d\ell}{B} = -\oint \frac{\delta B}{B^2} d\ell + \oint \frac{\delta(d\ell)}{B}. \tag{19.47}$$

End-point variations do not need to be considered in this closed-loop integral. Using equation (19.43) to relate $\delta(d\ell)$ to δB, we obtain

$$\delta \oint \frac{d\ell}{B} = -2 \oint \frac{\delta B}{B^2} d\ell. \tag{19.48}$$

Thus, in the limit of vanishing differentials, equation (19.46) reduces to

$$\left\langle \frac{d\theta}{dt} \right\rangle \propto \frac{d}{d\Phi} \oint \frac{d\ell}{B}. \tag{19.49}$$

Thus, the condition for instability, which corresponds to a *positive* value of $\langle d\theta/dt \rangle$, is that the quantity $\oint d\ell/B$ be *increasing outward.*

This is the simplest form of the stability condition for flute modes in closed field line configurations: in such configurations an isotropic-pressure plasma is stable or unstable depending on whether the quantity $\oint d\ell/B$ decreases or increases away from the center of the plasma; the integral is to be taken completely around a closed field line. Quadrupole configurations, such as that shown in Figure 19.8, can be made flute-stable according to this criterion.

The criterion for instability derived here, namely that $\oint d\ell/B$ must be increasing outward (i.e. in the direction opposite to that of the pressure-gradient vector), has applicability to a broader class of closed field line configurations than the axisymmetric (i.e. rotationally symmetric about the z axis) configurations discussed so far. Indeed, from the fluid viewpoint, this criterion could be obtained intuitively by considering whether a net expansion of the plasma occurs (thereby releasing kinetic energy) when flux tubes containing equal amounts of magnetic flux are interchanged. Consider a thin flux tube containing an amount $\delta\Phi$ of magnetic flux. At different points along this flux tube, its area δA is given by $\delta\Phi = B\delta A$, and so the volume of the entire flux tube is given by

$$\delta V = \oint \delta A \cdot d\ell = \delta\Phi \oint d\ell/B.$$

Now consider a 'rippling' perturbation of the plasma surface in which a plasma flux tube moves outward, while a 'vacuum flux tube' containing exactly the same

amount of magnetic flux moves inward; we could call this the 'interchange' of these two flux tubes. If the quantity $\oint d\ell/B$ is increasing outward, the plasma flux tube will expand as it moves outward, while the vacuum flux tube will contract as it moves inward. The overall effect will be a net expansion of the plasma and a reduction in its thermal energy, which then provides the energy needed to drive the instability.

It is clear from this discussion that these unstable flute perturbations do not occur only at a plasma–vacuum interface, but can occur interior to the plasma, in which case a flux-tube containing *high-pressure* plasma is interchanged with a flux-tube containing *lower-pressure* plasma. In this case, instability will occur if the quantity $\oint d\ell/B$ is increasing in the direction of lower plasma pressure (the equivalent of 'outward' in the case of a plasma–vacuum interface). As in the case of the gravitational Rayleigh–Taylor instability, we note that the release of energy is again second order in a displacement vector $\boldsymbol{\xi}$, since it scales as $-(\boldsymbol{\xi} \cdot \nabla p)[\boldsymbol{\xi} \cdot \nabla(\oint d\ell/B)]$.

One possible method for stabilizing the flute instability would be to add some 'shear' to the magnetic field. A magnetic field is said to be 'sheared' if the direction of the field vector rotates as one moves from one constant-pressure surface to the next. For example, in the quadrupole configuration shown in Figure 19.8, the addition of a B_θ component (e.g. by placing a current-carrying conductor along the z axis) would provide magnetic shear. In a sheared magnetic field, the interchange of two flux tubes cannot occur without 'twisting' the field lines, thereby increasing the magnetic energy. In this case, the energy made available by plasma expansion must compete with the increase required in the magnetic energy; this will generally impose a lower limit on the plasma β value for the instability to be possible.

Even in configurations that are flute-stable according to the $\oint d\ell/B$ criterion, e.g. the quadrupole configuration shown in Figure 19.8, there are generally regions along each field line where the magnetic curvature is unfavorable, i.e. concave towards the plasma. Although the flute instabilities discussed in this Chapter all extend uniformly along the entire length of the field lines (hence their name 'flutes'), it is clearly possible, in principle, for instabilities with the same driving mechanism to arise that are localized to finite regions of unfavorable curvature. Such instabilities will cause the plasma to 'balloon' outward along these finite portions of field lines. Conservation of magnetic flux then requires that the field lines 'bend', and this bending will generally increase the magnetic energy. As in the case of a sheared field, the energy made available by plasma expansion must compete with this increase in magnetic energy, and the instabilities—called 'ballooning instabilities'—also arise only above some threshold β value.

19.7 FLUTE INSTABILITY OF THE PINCH

Another configuration that is obviously susceptible to flute instabilities is the cylindrical 'self-pinched plasma' (see Chapter 9). Here, the magnetic field is produced by an axial current flowing in the plasma. The magnetic field is azimuthal (B_θ) and its radius-of-curvature is simply the radial coordinate r. Clearly, the field-curvature is always unfavorable (concave towards the plasma). In this case, the flute perturbations are azimuthal, as shown in Figure 19.10. From the shape of the perturbed plasma, this instability is sometimes called the 'sausage instability'.

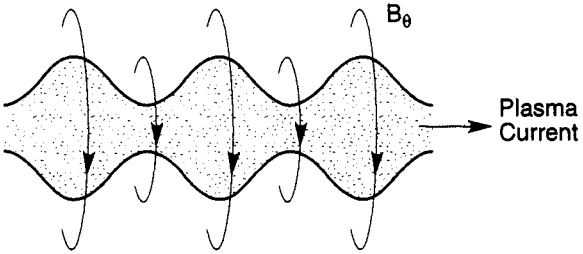

Figure 19.10. The flute, or 'sausage', instability of a self-pinched plasma.

The growth of the sausage instability is very rapid, since the radius-of-curvature of the field lines is effectively just the radius of the pinch column. From our previous formula, we estimate the growth rate to be

$$\gamma = \left(-\frac{2p'}{\rho r}\right)^{1/2} \tag{19.50}$$

where a prime denotes again a derivative with respect to the radial coordinate r.

19.8 MHD STABILITY OF THE TOKAMAK*

Before ending this Chapter, it may be useful to discuss very briefly the stability of the *tokamak* in the 'ideal MHD' model which has been used here to derive the Rayleigh–Taylor and flute instabilities. The tokamak configuration in the 'cylindrical approximation' was introduced in Chapter 9 and is illustrated in Figure 9.6. The actual tokamak geometry is toroidal, and the main magnetic field (corresponding to B_z in the cylindrical approximation) is toroidally directed, with the smaller magnetic field (B_θ in the cylindrical approximation) directed azimuthally the short way around the torus. The 'cylindrical tokamak' would clearly be vulnerable to flute instabilities, because the helical magnetic field produced by the combination of the B_z and B_θ fields has its curvature concave

toward the plasma. On the other hand, the field also has considerable magnetic shear, which we have seen to be a stabilizing effect. In the actual toroidal geometry, however, it turns out that the effect of the additional curvature introduced by 'bending' the cylinder into a torus generally dominates over the effect of the helical curvature in regard to the stability of flute modes. For a torus with major radius R, the toroidal curvature is favorable (convex toward the plasma) on the small-R side of the plasma and unfavorable (concave toward the plasma) on the large-R side. When a calculation is carried out for the actual toroidal geometry, the 'weighting' of the small-R side turns out to be slightly greater than the weighting of the large-R side, so the net effect of the toroidal curvature is stabilizing. For the net favorable toroidal curvature to exceed the unfavorable helical curvature (in the case of a tokamak of approximately circular plasma cross section), it is necessary only that $q \equiv rB_z/RB_\theta > 1$. In practice, the q value in a tokamak typically rises from about unity at the center of the plasma ($r = 0$) to three or higher at the plasma edge ($r = a$). Thus, this condition is usually satisfied in the tokamak, so that pure flutes are stable.

Following any helical field line around the torus, it is clear that the field line will alternately lie on the small-R and large-R sides of the plasma. Thus, as in the case of the closed field line quadrupole configuration shown in Figure 19.8, there are regions of favorable curvature and regions of unfavorable curvature on each field line; as we saw, this gives rise to the possibility of 'ballooning' instabilities. Since the field line makes exactly q transits the long way around the torus for each transit the short way around, these regions of favorable and unfavorable curvature are a distance of order qR apart along a field line. For a displacement ξ, the energy released per unit volume by a flute-like instability is of order $p'\xi^2/R$, whereas the energy per unit volume needed to bend the magnetic field over a distance of order qR (field-line bending being unavoidable for a ballooning instability, as distinct from a pure flute) is of order $(B_z^2/2\mu_0)(\xi^2/q^2R^2)$. Thus, ballooning instabilities will arise in tokamaks only when $p'/R > B_z^2/2\mu_0 q^2 R^2$, i.e. only for $\beta > \beta_{\text{crit}} \approx a/q^2R$, where we have estimated $p' \sim p/a$. This result should be taken only as a rough order-of-magnitude estimate: in practical cases, tokamaks tend to be stable to ballooning instabilities up to β values in the range 3–6%.

The tokamak can, however, exhibit an entirely different type of MHD instability, which is driven by the magnetic energy that is available in the tokamak magnetic field, rather than by the thermal energy that is available from plasma expansion. This instability, which can arise also in the cylindrical tokamak approximation, is called the 'kink', and it takes the form of a helical displacement of the plasma cylinder. The instability arises whenever such a perturbation lowers the magnetic energy of the B_θ field—the field component that is produced by currents in the plasma itself. In practice, kink instabilities tend to arise only at relatively low q values. We will not pursue them further

here, except to note that kinks are closely related (in regard to their source of energy) to a more slowly growing, but also more pervasive, instability that arises when resistivity is added to the MHD model. This instability, which occurs in many types of laboratory and naturally occurring plasmas in magnetic fields, is discussed in the next Chapter. For simplicity, we choose there to consider a simpler magnetic configuration (a plane current slab), which we find to be stable in the ideal MHD model.

The reader who is interested in pursuing further the topic of MHD instabilities in tokamaks is referred to J Wesson (1987 *Tokamaks* Oxford: Clarendon Press), or to R B White (1989 *Theory of Tokamak Plasmas* Amsterdam: North-Holland).